

Merrimack College

Merrimack ScholarWorks

Chemistry & Biochemistry Faculty Publications

Chemistry & Biochemistry

2008

Zeolite Activation of Organometallics: Revisiting Substitution Kinetics of $[\text{Mo}(\text{CO})_6]$ with Chemisorbed PMe_3 in Dehydrated Na_{56}Y Zeolite

Anthony L. Fernandez
Merrimack College, fernandeza@merrimack.edu

Jianbin Hao

Roberta L. Parkes

Anthony J. Poë

Eduardo J.S. Vichi

Follow this and additional works at: https://scholarworks.merrimack.edu/chm_facpub

 Part of the [Inorganic Chemistry Commons](#)

Repository Citation

Fernandez, A. L., Hao, J., Parkes, R. L., Poë, A. J., & Vichi, E. J. (2008). Zeolite Activation of Organometallics: Revisiting Substitution Kinetics of $[\text{Mo}(\text{CO})_6]$ with Chemisorbed PMe_3 in Dehydrated Na_{56}Y Zeolite. *Journal of the Brazilian Chemical Society*, 19(5), 862-871.
Available at: https://scholarworks.merrimack.edu/chm_facpub/1

This Article - Open Access is brought to you for free and open access by the Chemistry & Biochemistry at Merrimack ScholarWorks. It has been accepted for inclusion in Chemistry & Biochemistry Faculty Publications by an authorized administrator of Merrimack ScholarWorks. For more information, please contact scholarworks@merrimack.edu.

Zeolite Activation of Organometallics: Revisiting Substitution Kinetics of $[\text{Mo}(\text{CO})_6]$ with Chemisorbed PMe_3 in Dehydrated Na_{56}Y Zeolite

Anthony L. Fernandez,^{*a} Jianbin Hao,^b Roberta L. Parkes,^b Anthony J. Poë^{*b} and
(the late) Eduardo J. S. Vichi^{c,†}

^aDepartment of Chemistry, Merrimack College, 315 Turnpike Street, North Andover, MA 01845, USA

^bLash Miller Chemical Laboratories, University of Toronto, 80 St. George Street, M5S 3H6 Toronto, Canada

^cInstituto de Química, Universidade Estadual de Campinas, CP 6154, 13083-970 Campinas-SP, Brazil

Reações de $[\text{Mo}(\text{CO})_6]$ sob vácuo em cavidades α do zeólito Na_{56}Y totalmente carregadas com PMe_3 quimissorvido produzem *cis*- $[\text{Mo}(\text{CO})_4(\text{PMe}_3)_2]$, mas misturas de $[\text{Mo}(\text{CO})_5(\text{PMe}_3)]$ e *cis*- $[\text{Mo}(\text{CO})_4(\text{PMe}_3)_2]$ são produzidas sob CO. Reações sob vácuo exibem fatores entálpicos baixos e fatores entrópicos muito negativos ($\Delta H^\ddagger = 71,4 \pm 3,5 \text{ kJ mol}^{-1}$ and $\Delta S^\ddagger = -102 \pm 11 \text{ J K}^{-1} \text{ mol}^{-1}$), comparados com fatores entálpicos muito mais altos e fatores entrópicos positivos para reações de substituição dissociativa de CO por $\text{P}(n\text{-Bu})_3$ em xileno observadas em outros trabalhos. A reação a 66°C sob vácuo é cerca de 10^3 vezes mais rápida do que reações dissociativas ‘espontâneas’ de CO em solução. Conclui-se que a substituição intrazeólito ocorre por um mecanismo “assistido por zeólito” em que dois íons óxidos nas paredes da cavidade deslocam simultaneamente dois ligantes CO vizinhos do $[\text{Mo}(\text{CO})_6]$. Isso contrasta com valores de entalpia ainda menores e de entropia mais negativos para o deslocamento simultâneo de três ligantes CO vizinhos em reações de descarbonilação térmica. As cavidades α comportam-se como ligantes “zeolato” aniônicos multidentados, com números variáveis de íons O^{2-} participando da criação de estados de transição altamente ordenados. Os resultados enfatizam o alto grau com que estes estudos cinéticos podem revelar detalhes íntimos da natureza dos efeitos ativadores.

Reactions of $[\text{Mo}(\text{CO})_6]$ under vacuum in α -cages of Na_{56}Y zeolite fully loaded with chemisorbed PMe_3 form *cis*- $[\text{Mo}(\text{CO})_4(\text{PMe}_3)_2]$ but mixtures of $[\text{Mo}(\text{CO})_5(\text{PMe}_3)]$ and *cis*- $[\text{Mo}(\text{CO})_4(\text{PMe}_3)_2]$ are formed under CO. Reactions under vacuum exhibit low enthalpic and very negative entropic factors ($\Delta H^\ddagger = 71.4 \pm 3.5 \text{ kJ mol}^{-1}$ and $\Delta S^\ddagger = -102 \pm 11 \text{ J K}^{-1} \text{ mol}^{-1}$) compared with much higher enthalpic and positive entropic factors for CO dissociative reactions with $\text{P}(n\text{-Bu})_3$ in xylene observed elsewhere. Reaction at 66°C under vacuum is *ca.* 10^3 times faster than “spontaneous” CO dissociative reactions in solution. Intrazeolite substitution is concluded to occur by a “zeolite assisted” mechanism in which two oxide ions in the cavity walls simultaneously displace two neighbouring CO ligands from the $[\text{Mo}(\text{CO})_6]$. This contrasts with even lower enthalpy, and more negative entropy values, for simultaneous displacement of three neighbouring CO ligands in thermal decarbonylation reactions. The α -cages behave as multidentate anionic “zeolate” ligands with varying numbers of O^{2-} ions participating to create highly ordered transition states. These results emphasize the high degree to which such kinetic studies can reveal intimate details of the nature of these activating effects.

Keywords: hexacarbonylmolybdenum(0), Na_{56}Y zeolite, intrazeolite kinetics, PMe_3 substitution

[†] Professor Vichi sadly passed away just as this manuscript was being completed. Eduardo Vichi was the originator of the Intrazeolite Kinetics project. He suggested it to A.J.P. in Toronto in 1983 and eventually obtained funding for it through FAPESP and CNPq. He was a great scientific colleague and a warm friend, and he will be deeply missed.

*e-mail: anthony.fernandez@merrimack.edu; apoe@chem.utotonto.ca; anthonypoe@rogers.com

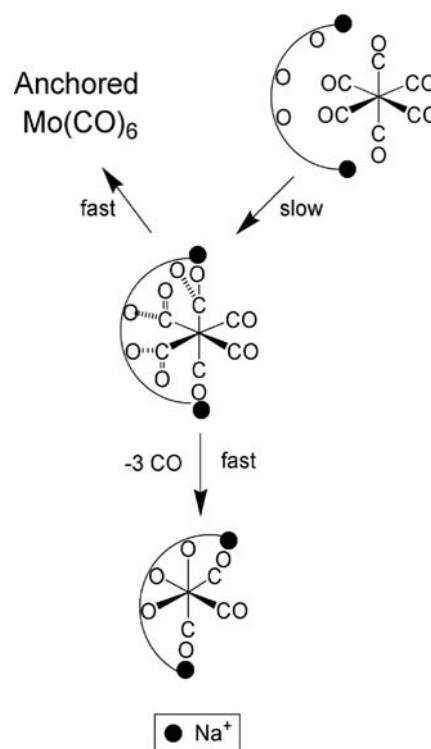
Introduction

The catalytic effect of zeolite cavities on many chemical reactions has been well known for over 60 years.¹ However, it was not until much later²⁻⁴ that the intrazeolite kinetics

of some simple stoichiometric reactions were reported, reactions that had previously been thoroughly studied in homogeneous solution and the gas phase.⁵ These reactions involved the ligand exchange reactions of $[\text{Mo}^{(12}\text{CO})_6]$ with ^{13}CO , and the substitution reactions of $[\text{Mo}(\text{CO})_6]$ with PMe_3 , all occurring within the α -cavities of dehydrated Na_{56}Y ($\text{Na}_{56}(\text{AlO}_2)_{56}(\text{SiO}_2)_{136}$). Preliminary studies of the reactions in other M_{56}Y zeolites were also reported.⁴ Apart from the detection³ of what were essentially bimolecular substitution reactions with physisorbed PMe_3 , a very striking observation was the very low activation enthalpy of the CO exchange reaction which was offset, but not overcome, by a substantially unfavorable activation entropy. The combined effect was to accelerate the reactions by a factor of ~ 1000 at 66°C , compared with those in homogeneous solution or in the gas phase.

Only one other study of such intrazeolite kinetics has been reported since then⁶ and this too involved substitution of PMe_3 into $[\text{Mo}(\text{CO})_6]$. Reactions were monitored by NMR techniques at low loadings of PMe_3 (≤ 2 molecules PMe_3 per alpha cage), a region where minimal studies had been carried out previously.³ A closely related important study of kinetics of adsorption and decarbonylation reactions of $[\text{Mo}(\text{CO})_6]$ on the surfaces of hydroxylated or partially dehydroxylated alumina has also been described.⁷

A recent account⁸ of the thermal decarbonylation kinetics of $[\text{Mo}(\text{CO})_6]$ in Na_{56}Y revealed even lower activation enthalpies, and even more negative activation entropies than the ^{13}CO exchange reactions. This, and the direct formation of the subcarbonyl $[\text{Mo}(\text{CO})_3]$, coordinated by three neighboring oxide ions in the cavity walls, was taken to indicate that the rate determining step involved a concerted attack by those oxide ions on the carbon atoms of three *fac* CO ligands (Scheme 1). This conclusion differed from that previously reached²⁻⁴ where interaction between the Na^+ ions and the oxygen atoms of the CO ligands was considered the source of activation. However, the same rate determining step, to form a common intermediate, was implied for the reactions of the undissociated $[\text{Mo}(\text{CO})_6]$ in which it became “anchored” within a “12-ring window” between two alpha cages in the zeolite by as many as six sodium ions.⁹ The activation parameters for CO exchange, and tentative values for PMe_3 substitution (but under not very well defined conditions³), lay between those for reaction in solution and those for replacement of three CO ligands and a study of the substitution reactions to form *cis*- $[\text{Mo}(\text{CO})_4(\text{PMe}_3)_2]$ under precisely defined conditions seemed desirable. We therefore report here a detailed study of the temperature dependence of the substitution reactions of $[\text{Mo}(\text{CO})_6]$ with well defined loadings of chemisorbed PMe_3 . It is



Scheme 1.

concluded that, in these reactions, only two oxide ions are involved in the activation process.

Extensive theoretical, spectroscopic and other non-kinetic material relating to structures and reactions of encapsulated organometallics is available that provides a background against which the results of kinetic studies can be assessed, and a collection^{3,4,9,10} includes original papers and reviews.

Experimental

Chemicals and instruments

High purity, crystalline Na_{56}Y with the unit cell composition $\text{Na}_{56}(\text{AlO}_2)_{56}(\text{SiO}_2)_{136} \cdot x\text{H}_2\text{O}$ was donated to Professor Geoffrey Ozin (of the Chemistry Department at the University of Toronto – U. of T.) by Dr. Edith Flanigen, then at UOP, Tarrytown, NY, some years ago, and kindly passed on to us. $[\text{Mo}(\text{CO})_6]$ (Strem), carbon monoxide (BOC, grade 2.3) and the adduct (trimethylphosphine)silver iodide $\{(\text{PMe}_3)_3\text{AgI}\}_4$ (Aldrich) were used as received. The IR spectra were recorded with a Nicolet Magna 550 FTIR spectrophotometer. Spectra during reactions were automatically recorded at specified times using Omnic[®] software, which allowed for the automation of data collection using a self-written macro program. The reaction cell, designed by Professor Ozin, has been fully

described elsewhere.³ It includes a stainless steel reaction chamber, embedded in a temperature controlled furnace, and connected to a quartz tube where pre-treatments are carried out.³ The chamber is arranged so that zeolite samples, contained in a stainless steel holder, can be positioned precisely between the air cooled CaF_2 windows of the reaction chamber, which is in turn positioned in the beam of the spectrophotometer.

Kinetic studies

The procedures for studying the reaction kinetics were exactly the same as described elsewhere.³ The Na_{56}Y was stored at constant humidity and its crystallinity was checked by powder X-ray diffraction by Dr. S. Petrov in the Chemistry Department of the University of Toronto.

The spectrum of the dehydrated zeolite was recorded to provide a base line for further spectroscopic measurements. Successive samples of $[\text{Mo}(\text{CO})_6]$ were sublimed into the zeolite wafer until absorbances were generally between 1 and 2 units (*ca.* 1 - 2 molecules per unit cell, or 0.1-0.3 *per* α -cavity³). The sample was then briefly heated under static vacuum to remove any residual $[\text{Mo}(\text{CO})_6]$ that had not become fully encapsulated within the zeolite. The $(\text{PMe}_3 \cdot \text{AgI})_4$ was then loaded into a side arm of the reaction cell in amounts that would lead eventually to complete saturation of the zeolite with chemisorbed PMe_3 , and with some physisorbed PMe_3 as well. The side arm was evacuated and opened up to the reaction cell so that PMe_3 could be loaded into the zeolite wafer by gentle heating of the adduct for *ca.* 10 min. The wafer was then left under vacuum for *ca.* 20 min so that all physisorbed PMe_3

was removed and the zeolite was fully loaded only with chemisorbed PMe_3 , there being four phosphine molecules in each α -cage not occupied by a chemisorbed $[\text{Mo}(\text{CO})_6]$ molecule, and two in each α -cage that was occupied by one $[\text{Mo}(\text{CO})_6]$ molecule.³ Physisorbed and chemisorbed PMe_3 are distinguished, by definition, on the basis of the former being removable in this way under vacuum while the latter is not. When required, the cell was then charged with CO (650 Torr) which had been passed through a tube filled with Drierite, and this procedure necessitated removal of the reaction cell from the spectrophotometer.

Reconnection to the spectrophotometer allowed for monitoring the subsequent reactions by recording spectra at pre-selected times after the required temperature had been attained. The time-dependent spectra, and absorbance changes at chosen wave numbers, were collected automatically so that they could be stored and manipulated as required. The absorbance changes were easily fitted to single or double exponential functions that provided values of rate constants (k_{obs}) for the first stage of the reaction. Derivation of activation parameters was effected by standard Eyring analyses.

Results

Spectroscopic changes under vacuum

Spectra recorded immediately after the introduction of the $[\text{Mo}(\text{CO})_6]$ showed a single, rather unsymmetrical, broad band at 1972 cm^{-1} , a weak band at 2123 cm^{-1} , and poorly resolved shoulders at ~ 1900 and 2050 cm^{-1} (Figure 1). Loading of PMe_3 showed clear bands at $2965(\text{s})$,

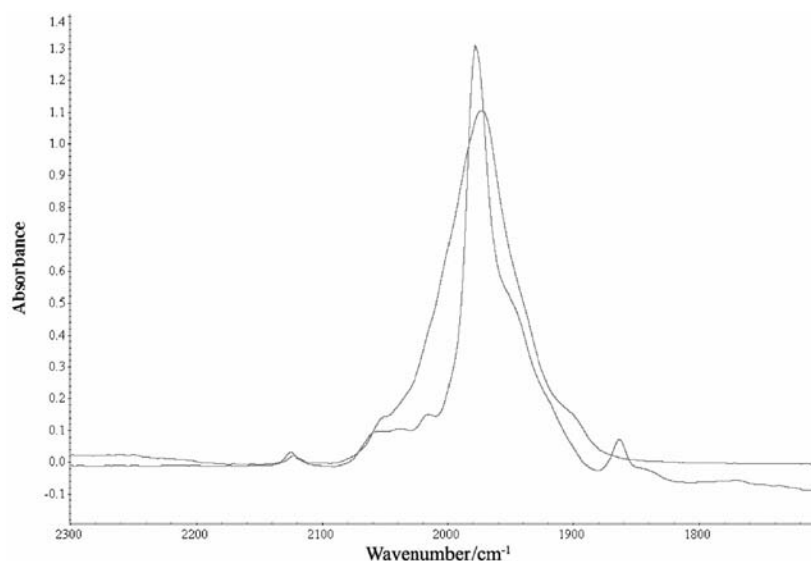


Figure 1. Mid IR spectrum of $[\text{Mo}(\text{CO})_6]$ in Na_{56}Y (a) (broad band) before and (b) (sharper band) after introduction of PMe_3 . The weak band at 1865 cm^{-1} in the latter spectrum shows that a small amount of reaction had occurred by the time the spectrum was measured.

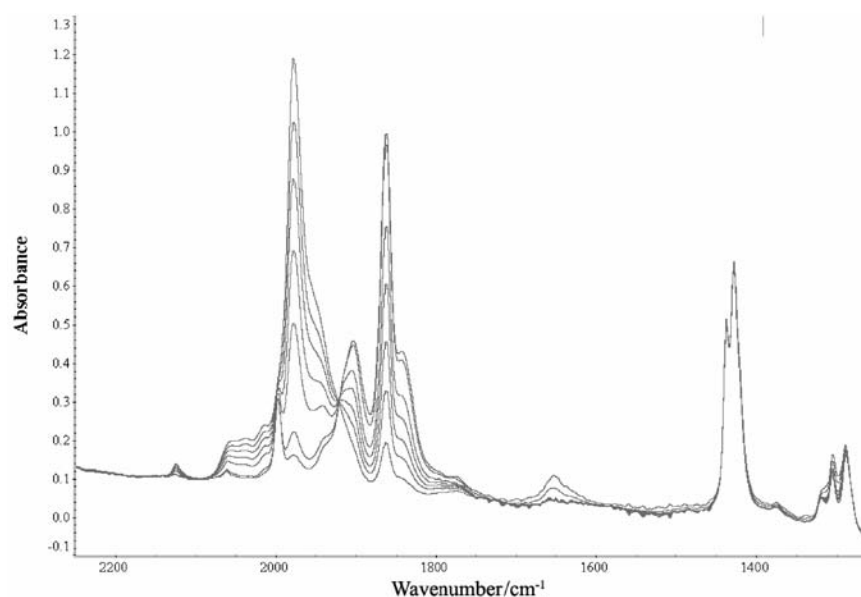


Figure 2. Time-dependent spectra during reactions of $[\text{Mo}(\text{CO})_6]$ in Na_{36}Y saturated with chemisorbed PMe_3 , *i.e.* 2 molecules PMe_3/α cage occupied by an $[\text{Mo}(\text{CO})_6]$ molecule, and 4 molecules/ α cage not occupied by an $[\text{Mo}(\text{CO})_6]$ molecule, under vacuum at 48 °C, taken at times $10^{-3} t = 0, 2.46, 5.17, 9.50, 15.93, 39.21,$ and 58.77 s. The band at 1975 cm^{-1} is decreasing in absorbance, and those at $1905, 1865$ and 1645 cm^{-1} are increasing.

$2900(\text{vs}), 2845(\text{vw}),$ and $2820(\text{w}),$ a pair of quite strong bands at 1440 and $1430,$ and a group of weaker bands at $1320, 1305$ and $1290\text{ cm}^{-1},$ all due to the $\text{PMe}_3.$ In addition the band at 1972 cm^{-1} had become much sharper (Figure 1), thereby revealing a weakly resolved band at $2017\text{ cm}^{-1},$ and a shoulder at *ca.* $1950\text{ cm}^{-1}.$ The main band had moved up in energy slightly to $1975\text{ cm}^{-1}.$ In the process of loading the PMe_3 some reaction leading to a band at $1865\text{ cm}^{-1},$ with a shoulder at *ca.* $1842\text{ cm}^{-1},$ had occurred (see below).

After the temperature had equilibrated, the spectra changed steadily as shown in Figure 2 by a selection (*< ca.* 1 in 10) from the many available spectra. The final spectrum showed sharp bands at $2000, 1905$ and $1865,$ and a shoulder at $1845\text{ cm}^{-1}.$ This spectrum is identical with that observed previously and assigned,³ on spectroscopic and other evidence, to *cis*- $[\text{Mo}(\text{CO})_4(\text{PMe}_3)_2].$ The intensities of the product bands usually declined slightly over extended reaction times but, before the decrease became evident, there was a sharp isosbestic point at 1923 cm^{-1} and this occurred at that same wave number at all temperatures used. The intensities of the bands at $2900\text{--}2800, 1440$ and 1430 cm^{-1} that are assigned to the chemisorbed PMe_3 were constant from run to run (allowing for slight variations in the mass of the zeolite) and were largely unaffected over the course of the reaction. (The bands at $2900\text{--}2800\text{ cm}^{-1}$ are not shown in Figure 2 so that the changes at lower wavenumbers can be more clearly illustrated.) The bands at $1320\text{--}1290\text{ cm}^{-1}$ did occasionally show some minor changes. Finally, a

weak band at *ca.* $1650\text{ cm}^{-1},$ assignable to adsorbed water molecules,^{11,12} also grew during the course of the reaction, but only over the later stages. Thus, in the run shown in Figure 2, it had barely grown in at all after 75% reaction, and had reached only half its maximum intensity after *ca.* 90% reaction. Maximum absorbances corresponded to less than *ca.* 1 molecule/ α cage¹¹ and the absorbances were much less at higher temperatures.

Spectroscopic changes under 650 Torr CO

As with reactions under vacuum, spectra recorded immediately after the sublimation of PMe_3 include the bands due to $\text{PMe}_3,$ but two broad bands characteristic of CO also show clearly at 2175 and $\sim 2120\text{ cm}^{-1}.$ The lower energy band obscures the weak bands on the high energy side of the main band due to $[\text{Mo}(\text{CO})_6]$ at $1975\text{ cm}^{-1}.$ The absorbances of the bands due to CO remain constant throughout the reactions, and from run to run.

Upon heating to between 48 and 85 °C the spectra underwent very clean IR spectral changes as illustrated by the selection of spectra in Figure 3. As with reactions under vacuum, bands due to PMe_3 at $2900\text{--}2800$ (not shown for reasons given above), 1440 and 1430 cm^{-1} showed no change at all over the course of the reactions. However, the three weaker bands at $1320, 1306,$ and 1290 cm^{-1} showed rather more changes, and a fairly weak band at 1365 cm^{-1} grew in. Bands due to adsorbed water molecules also grew in, to a greater extent than in the reactions under vacuum,

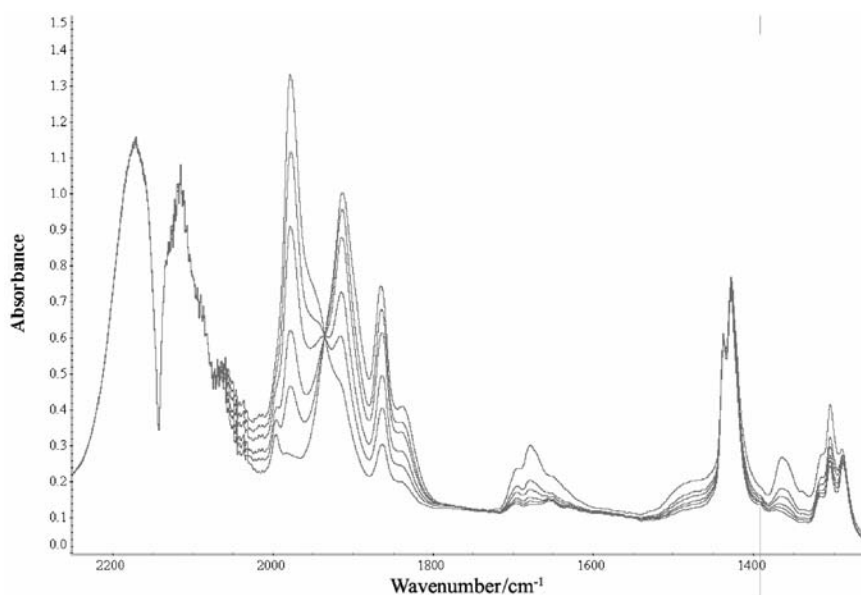


Figure 3. Time-dependent spectra during reactions of $[\text{Mo}(\text{CO})_6]$ in Na_{56}Y saturated with chemisorbed PMe_3 under 650 Torr CO at 75 °C, taken at times $10^{-3} t = 0, 0.450, 1.01, 2.29, 3.75$ and 12.51 s. The band at 1975 cm^{-1} is decreasing in absorbance, and those at $1913, 1865$ and 1645 cm^{-1} are increasing.

but by the end of the reactions there were only *ca.* 1-2 molecules/ α cage.¹¹

The growth of strong bands at 1913 and 1865 cm^{-1} coincided with the decline at 1975 cm^{-1} and continued to the end of the reaction. A weak band at 1995 cm^{-1} and shoulders at 1935 and 1840 cm^{-1} also grew. A sharp isosbestic point occurred at *ca.* 1935 cm^{-1} and was unaffected by the temperatures at which the runs were carried out. The bands at 1865 and 1995 cm^{-1} can be assigned to formation of the *cis*- $[\text{Mo}(\text{CO})_4(\text{PMe}_3)_2]$ as before,³ while the band at 1913 cm^{-1} and the shoulder at 1935 cm^{-1} can be assigned to $[\text{Mo}(\text{CO})_5(\text{PMe}_3)]$,² both complexes showing a downward shift of $\sim 30\text{-}35\text{ cm}^{-1}$ in NaY , compared to their bands in solution. These shifts are comparable with the slightly smaller shift of *ca.* 15 cm^{-1} shown by the hexacarbonyl on encapsulation in NaY .¹³ The ratios of *mono* to *bis* products can only be estimated approximately from the spectra but *ca.* 60 – 70% yields of $[\text{Mo}(\text{CO})_5(\text{PMe}_3)]$ are indicated, independent of temperature.

The kinetics of reaction

The clean IR spectral changes, with sharp isosbestic points, led to typical kinetic traces as shown in Figures 4 and 5. Rate constants were obtained by monitoring the decrease in the band at 1975 cm^{-1} and the increase in the bands at 1865 cm^{-1} , the band common to the reaction products under vacuum and under CO. The absorbance decreases at 1975 cm^{-1} were fitted closely by single exponential functions

(Figure 4) but the growth of absorbances at 1865 cm^{-1} under vacuum was often better analyzed by double exponential fitting because of the gradual decay of the products (Figure 4). This was not sufficiently pronounced to affect the appearance of the isosbestic points over large periods of the reactions and the problem was less apparent for reactions

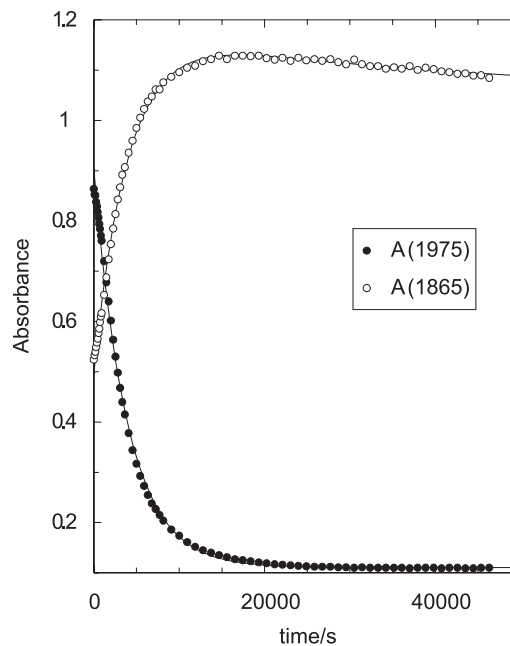


Figure 4. Kinetic traces for the decrease of absorbance at 1975 cm^{-1} , and the increase at 1865 cm^{-1} , for a reaction of $[\text{Mo}(\text{CO})_6]$ with chemisorbed PMe_3 in Na_{56}Y under vacuum at 66 °C. $10^4 k_{1975} = 2.56 \pm 0.03\text{ s}^{-1}$ and $10^4 k_{1865} = 2.50 \pm 0.09\text{ s}^{-1}$.

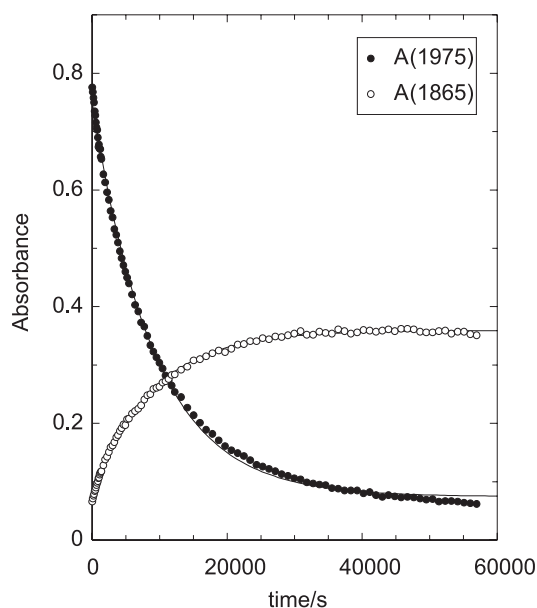


Figure 5. Kinetic traces for the decrease in absorbance at 1975 cm^{-1} , and the increase at 1865 cm^{-1} , for a reaction of $[\text{Mo}(\text{CO})_6]$ with PMe_3 in Na_{56}Y under 650 Torr CO at 56 $^\circ\text{C}$. $10^4k_{1975} = 1.10 \pm 0.01 \text{ s}^{-1}$ and $10^4k_{1865} = 1.14 \pm 0.01 \text{ s}^{-1}$.

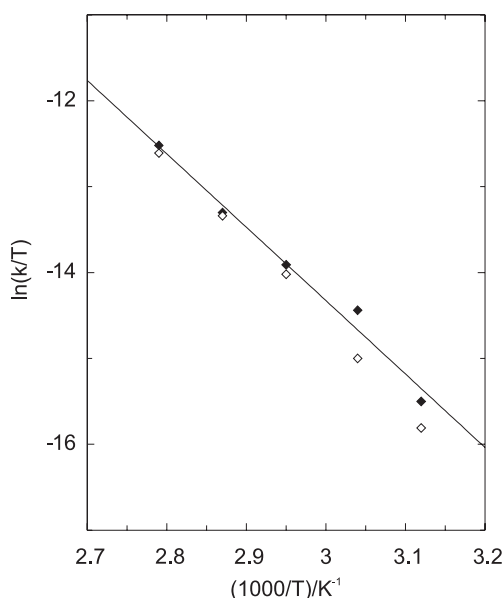


Figure 6. Eyring plot for average rate constants under vacuum (filled diamonds) and under 650 Torr CO (open diamonds). The line is the least squares line drawn through the data for reactions under vacuum.

under CO. First order rate constants are shown in Table 1, and the corresponding Eyring plots are shown in Figure 6. The activation parameters are included in Table 2.

Discussion

The very clean spectroscopic changes, and the rate data obtained from them, show that such studies can provide a

Table 1. Rate constants for substitution of PMe_3 into $[\text{Mo}(\text{CO})_6]$ in Na_{56}Y^a

$T/^\circ\text{C}$	$10^4k_{\text{obs}}/\text{s}^{-1}$ (under vacuum) { $N,^b \sigma(k_{\text{obs}})^c$ }	$10^4k_{\text{obs}}/\text{s}^{-1}$ (under 650 Torr CO) { $N,^b \sigma(k_{\text{obs}})^c$ }	$k_{\text{co}}/k_{\text{vac}}$
48.0	0.595 ± 0.040 {6, 17%}	0.436 ± 0.024 {8, 16%}	0.73 ± 0.06
56.0	1.77 ± 0.14 {6, 19%}	1.01 ± 0.11 {12, 38%}	0.57 ± 0.08
66.0	3.08 ± 0.23 {10, 24%}	2.76 ± 0.30 {6, 27%}	0.90 ± 0.12
75.0	5.80 ± 0.45 {3, 13%}	5.62 ± 0.40 {3, 12%}	0.97 ± 0.10
85.0	13.1 ± 1.0 {5, 17%}	11.9 ± 0.3 {2, -}	0.91 ± 0.07

^a Obtained from the decrease of absorbance at 1975 cm^{-1} or the growth of absorbance at 1865 cm^{-1} (see Table S1). ^b Number of determinations. ^c Estimated standard deviation of an individual rate constant in each set. A standard deviation of 24% is obtained from the pooled variances of all 61 individual values.

Table 2. Activation parameters for reactions of $[\text{Mo}(\text{CO})_6]$

Reaction	$\Delta H^\ddagger/\text{kJ mol}^{-1}$	$\Delta S^\ddagger/\text{J K}^{-1} \text{mol}^{-1}$	$\sigma(k_{\text{obs}})/\%b$
Dissociative substitution reaction with $\text{P}(n\text{-Bu})_3$ in decalin solution ^{5,8}	133 ± 6	28 ± 16	
^{13}CO exchange in Na_{56}Y^2	61.5 ± 5.0	-139 ± 13	15
PMe_3 substitution reactions under vacuum ^a	71.4 ± 3.8	-102 ± 11	27
$[\text{Mo}(\text{CO})_6]$ anchoring under vacuum ⁸	41.4 ± 3.0	-181 ± 9	22
$[\text{Mo}(\text{CO})_6]$ decarbonylation under vacuum ⁸	39.0 ± 2.9	-189 ± 9	22

^a This work. Estimated using all rate constants individually (see SI, Tables S1 and S2). ^b Estimated standard deviation of an individual rate constant.

good methodology for investigating the activating effects of zeolitic environments on model organometallic reactions under closely controlled conditions. The sharpness of the isosbestic points and the closeness of fit of the absorbance changes to single-exponential functions, over at least the major part of the reactions, show that individual reactions are kinetically well enough behaved that probabilities of reaction (*i.e.* the rate constants) do not change *during* the reactions. However, the reproducibility of the rate constants is less than is commonly observed for reactions in homogeneous solution. Thus, the data in Table 1 show that standard deviations of individual rate constants in a given set, estimated from their scatter around the averages,

rise from *ca.* 12% to as much as 38% for a single set of data. Pooling the variances from all 61 rate constants leads to a value of 24%. Similar values were found when all the individual rate constants were used in Eyring analyses (Table 2), and previous studies^{2-4,8} led to comparable values. This relatively low reproducibility is evidently a function of the nature of the zeolitic environment and should not be surprising.

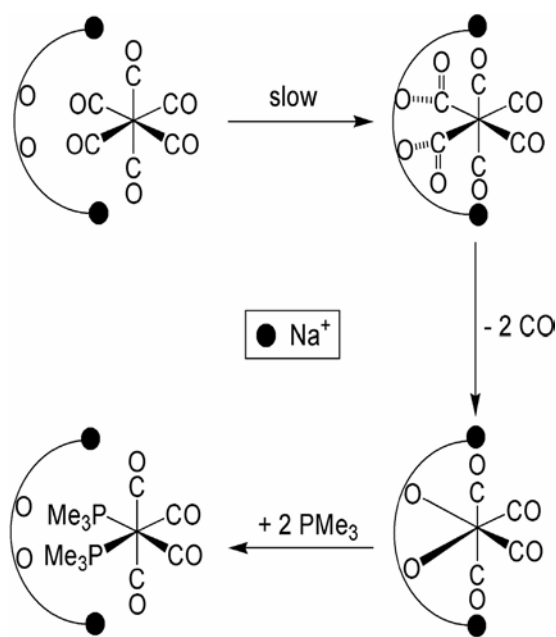
In this respect it must be recognized that each carbonyl molecule is confined in a zeolite cavity together with two PMe_3 molecules attached to two Na^+ ions not already blocked by the carbonyl. These individual "agglomerates" have a given probability of reaction, expressed as a first order rate constant, in events per unit time, and the reaction can be considered to be essentially an intramolecular reaction of the agglomerate. The question of concentration does not arise in these circumstances except in so far as variable loading changes the overall environment of the agglomerate. When that particular carbonyl has reacted the $[\text{Mo}(\text{CO})_6]$ has been replaced by a product molecule and it is left to other unsubstituted carbonyl molecules to undergo *their* reactions.

Thus it is possible that some non-uniformity in the composition of the NaY, and accompanying changes in Si:Al and Na:Si ratios, may contribute to the rather low reproducibility, and irregular distribution of reactant carbonyl molecules may operate as well. That this could produce the observed effects is suggested by the fact that significant changes in rates of substitution at 66 °C were caused by increased loading of the $[\text{Mo}(\text{CO})_6]$.³ Other evidence, such as the observed decrease in rates of displacement of ^{12}CO in $[\text{Mo}(^{12}\text{CO})_6]$ by ^{13}CO as the pressure of ^{13}CO increased, and the reduced rates of displacement of CO from $[\text{Mo}(\text{CO})_6]$ by chemisorbed PMe_3 as the loading of PMe_3 increased, all show the sensitivity of rates to the details of the environment.³ Significant kinetic effects were therefore transmitted through the zeolite framework even by the presence of such apparently innocuous species as CO, which in fact had a larger effect than the PMe_3 . These considerations may also explain the differences between the rate constants observed here and those found, under much lower PMe_3 loadings and by NMR monitoring techniques,⁶ and this is not to mention the common differences frequently observed between rate constants obtained from absorbance decreases and increases, the latter being more variable owing to the greater uncertainty in A_∞ values.

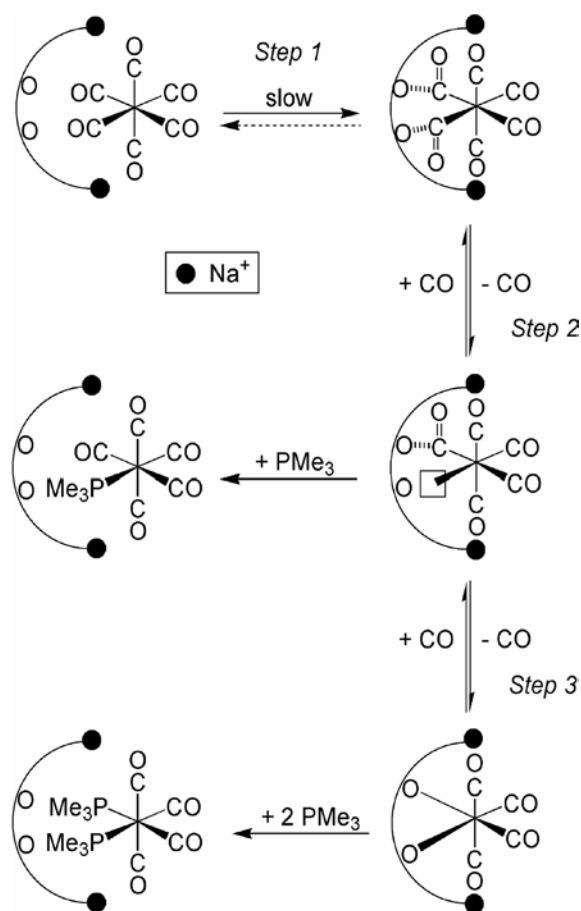
However, the large numbers of independent rate constants derivable from the data, and the large (almost 40 °C) temperature range involved, suffice to ensure that quite precise activation parameters are obtained

even if individual rate constants are not highly precise. The activation parameters will reflect the enthalpies and entropies pertaining to an *average* environment. This is particularly relevant when considering the significance of the very large differences between the parameters for different reactions (see Table 2).

In this particular study it is found that the activation parameters for intrazeolite substitution reactions under vacuum are very close to those found previously^{2,3} for the ^{13}CO exchange reaction with $[\text{Mo}(^{12}\text{CO})_6]$ at 110 Torr ^{13}CO . An exact agreement would not be expected because the rates depend on the pressure of ^{13}CO or the loading of PMe_3 . The new activation parameters for substitution are also close to the tentative ones previously derived by making some quite significant assumptions regarding the effects on the rate constants of different loadings of PMe_3 .³ The enthalpy values are considerably less (*ca.* 70 kJ mol^{-1}) than those for the reactions in homogeneous hydrocarbon solutions or even in the gas phase.⁵ However, this contribution to the activation is offset by considerably negative activation entropies which contribute *ca.* 50 kJ mol^{-1} unfavourably to the free energy of activation at *ca.* 70 °C. On the other hand, the activation parameters for the loss of three CO ligands, and the parallel anchoring in the windows between the alpha cages, show an even lower activation enthalpy and an even more negative activation entropy.⁸ The latter was rationalized by the proposal that three neighbouring oxide ions in the inner surfaces of the zeolite become attached to the carbon atoms of three *fac* CO ligands as shown in Scheme 1. This reduces the activation enthalpy, due to coincident formation of three bonds, but reduces the entropy because of the very restricted nature of the transition states. This led to the suggestion⁸ that the intrazeolite ^{13}CO exchange reaction was intermediate between the unrestricted reactions in homogeneous solution and the tightly prescribed decarbonylation and anchoring intrazeolite reactions, but much closer to the latter. And the facts that the activation enthalpies were higher, and the activation entropies were significantly less negative, than for decarbonylation or anchoring, were significant and indicative of a mechanism in which only two oxide ions were involved in activating two neighbouring CO ligands, rather than three. An identical process for the reactions with PMe_3 is shown in Scheme 2, where the activation and loss of two CO ligands is followed by addition of two PMe_3 molecules to form the *cis*-, disubstituted $[\text{Mo}(\text{CO})_4(\text{PMe}_3)_2]$ product. Apart from the fact that the activation parameters for the substitution reactions with precisely defined loadings of chemisorbed PMe_3 are very close to those for the ^{13}CO exchange reactions, the participation of two oxide ions



Scheme 2.



Scheme 3.

is supported by the formation of the *cis* complex as the only product under vacuum. The effective participation of oxide ions in this way is fully in accord with the well known susceptibility of the C atoms in CO ligands to attack by “hard” nucleophiles such as ^-OR , N_3^- etc.¹⁴

At all temperatures the presence of an atmosphere of 650 Torr CO leads to formation of substantial amounts of monosubstituted $[Mo(CO)_5(PMe_3)]$ in addition to *cis*- $[Mo(CO)_4(PMe_3)_2]$. However, under the conditions we have used, the rates are not appreciably affected, except at lower temperatures when they are reduced only slightly (Figure 6 and Table 1). Previous studies showed a rather larger retarding effect of CO,³ but the various sets of experiments reported here were carried out independently by several different experimenters over an extended period. We are confident that they represent a true picture of the effects of the average environment provided by the zeolite.

The stability of the *cis*- $[Mo(CO)_4(PMe_3)_2]$ at the end of the reaction shows that the $[Mo(CO)_5(PMe_3)]$ cannot be formed by displacement of PMe_3 from the former by CO. This suggests that the loss of the two CO ligands from the first intermediate in Scheme 2 is stepwise and not concerted, and the sequence of reactions outlined in Scheme 3 is consistent with the kinetic and yield data.

The following points are important. Step 1 has to be rate determining, with step 2 being much faster to avoid sufficient accumulation of the first intermediate for it to be observable. Step 2 must be reversible, and Step 1 is also probably slightly reversible, because an atmosphere

of 650 Torr CO does reduce the rate detectably at lower temperatures (see Table 1). If Step 1 were completely irreversible then no amount of reversibility of Step 2 could reduce the rate. This reversibility of Step 1 could be caused by the greater accumulation of the first intermediate when reactions are carried out under CO.

The intermediate formed in Step 2 has a vacant coordination site, one that can be irreversibly filled by PMe_3 or reversibly filled by CO in Step 3. This reversibility means that the relative yield of $[Mo(CO)_5(PMe_3)]$ can be enhanced because the net rate of CO loss is decreased so that PMe_3 addition can compete with it.

The fact that $[Mo(CO)_5(PMe_3)]$ does not undergo activation of two *cis* CO ligands and react further to form a trisubstituted product is most probably due to a combination of steric restrictions and the lower electron affinity of the C atoms in the CO ligands due to the high basicity of the PMe_3 ligand already present.

Finally, the negligible effect of the appearance, due probably to minor leaks in the vacuum system, of a small number of water molecules during many of the reactions is of interest. These H_2O molecules are expected to become

attached to sodium ions so that an activation process involving only or mainly attachment of the [Mo(CO)₆] to these cations would be expected to lead to considerable rate inhibition. The fact that this is not observed, and that even the deliberate addition of water molecules has only minor effects,¹⁵ serves to support the importance in the activation process of the oxide ions, rather than the Na⁺ ions as previously postulated.² There have been other indications of the negligible effect of water molecules as shown by the nature of products in such situations.¹⁶ The importance of the high electric fields associated with the bare cations in the surface of the cavities may therefore be less than previously envisaged.⁴

However, there is a pronounced sharpening (shown in Figure 1) of the 1975 cm⁻¹ band of the [Mo(CO)₆] upon introducing the PMe₃, but before significant reaction occurs. This does indicate an initial interaction of the [Mo(CO)₆] with the Na⁺ ions, and a lessening of that influence, consequent on the competing bonding of the PMe₃ to Na⁺ ions.

Conclusions

These results confirm that intrazeolite kinetics studies of model organometallic reactions are perfectly feasible. Reactions are stoichiometrically well defined and reproducible although the rate constants obtained may suffer from minor reproducibility problems. However, the activation parameters relevant to average reactant environments can provide indications of significant differences in mechanism between different reactions, revealing intimate details of the various activating processes that zeolitic encapsulation can provide. Thus, the negligible effect of the presence of water molecules, and the essential participation of the oxide ions from the interior surface of the zeolite cavities can be established, as well as the number participating in particular reactions. Extension to studies of reactions of related metal carbonyls and metal carbonyl clusters enclosed in zeolites with different metal ions and Si:Al ratios is likely to be of interest and the paucity of such studies remains surprising.

Acknowledgements

We gratefully acknowledge the Petroleum Research Fund, administered by the American Chemical Society, and the Natural Sciences and Engineering Research Council of Canada for financial support. We are also grateful for financial support from the FAPESP during his sabbatical leave (E. J. S. V.) and to CNPq for support via the PRONEX project.

Supplementary Information

Rate constants for individual runs under vacuum and under 650 Torr CO are given in Tables S1 and S2, which are available free of charge at <http://jbcs.sbj.org.br>, as a PDF file.

References

1. Barrer, R. M.; U. S. Pat. 2,306,610 **1941**; Bein, T. In *Comprehensive Supramolecular Chemistry*, Lehn, J. -M.; Atwood, J. L.; Davies, J. E. D.; MacNicol, D. D.; Vogtle, F., eds.; Pergamon, Oxford U.K., 1966, Vol. 7, ch. 20; Vaughan D. E. W. In *Comprehensive Supramolecular Chemistry*, Lehn, J. -M.; Atwood, J. L.; Davies, J. E. D.; MacNicol, D. D.; Vogtle, F., eds.; Pergamon, Oxford U.K., 1966, Vol. 7, ch. 13.
2. Ozin, G. A.; Özkaz, S.; Pastore, H. O.; Poë, A. J.; Vichi, E. J. S.; *J. Chem. Soc., Chem. Comm.* **1991**, 141.
3. Pastore, H. O.; Ozin, G. A.; Poë, A. J.; *J. Am. Chem. Soc.* **1993**, *115*, 1215.
4. Ozin, G. A.; Öskar, S.; Pastore, H. O.; Poë, A. J.; Vichi, E. J. S.; *ACS Symp. Ser.* **1992**, No. 499, 314.
5. Howell, J. A. S.; Birkinshaw, P. M.; *Chem. Rev.* **1983**, *83*, 557; Angelici, R. J.; Graham, J. R.; *J. Am. Chem. Soc.* **1966**, *88*, 3658; Angelici, R. J.; Graham, J. R.; *Inorg. Chem.* **1967**, *6*, 2082.
6. Hu, S.; Apple, T.; *J. Phys. Chem.* **1994**, *98*, 13665.
7. Reddy, K. P.; Brown, T. L.; *J. Am. Chem. Soc.* **1995**, *117*, 2845.
8. Fernandez, A. L.; Hao, J.; Parkes, R. L.; Poë, A. J.; Vichi, E. J. S.; *Organometallics* **2004**, *23*, 2715. (N.B. The reference 16b in Table 2 of this reference should have been 10b.)
9. Brémard, C.; *Coord. Chem. Rev.* **1988**, *178-180*, 1647; Brémard, C.; Ginestet, G.; Laureyans, J.; Le Maire, M.; *J. Am. Chem. Soc.* **1995**, *117*, 9274.
10. Yokota, T.; Yaginuma, M.; Kondo, J. N.; Domen, K.; Hirose, C.; Wakabayashi, F.; *Catal. Lett.* **1996**, *40*, 89; Grey, C.; Poshni, F. L.; Gualtieri, A. F.; Norby, P.; Hanson, J. C.; Corbin, D. R.; *J. Am. Chem. Soc.* **1997**, *119*, 1981; Shen, G.-C.; Liu, A. M.; Ichikawa, M.; *J. Chem. Soc., Faraday Trans.* **1998**, *94*, 1353; Okamoto, Y.; Kubota, T.; *Microporous Mesoporous Mater.* **2001**, *48*, 301; Yamaguchi, A.; Sususki, A.; Shido, T.; Inada, Y.; Asakura, K.; Nomura, M.; Iwasawa, Y.; *J. Phys. Chem. B* **2002**, *106*, 2415; Huang, Y.; Poissant, R. R. *Langmuir* **2002**, *18*, 5487; Lee, F.; Gates, B. C.; *J. Phys. Chem. B* **2004**, *108*, 11259.
11. Fernandez, A. L.; Poë, A. J., unpublished work.
12. Bertsch, L.; Habgood, H. W.; *J. Phys. Chem.* **1963**, *67*, 1621. (The journal cited here was inadvertently given as *Can. J. Chem.* in reference 8).

13. Poilblanc, R.; Bigorgne, M.; *Bull. Chem. Soc. de France* **1962**, 1301; Smith, J. G.; Thompson, D. T.; *J. Chem. Soc. A* **1967**, 1694; Jenkins, J. M.; Verkade, J. G.; *Inorg. Chem.* **1967**, 6, 2250; Bor, G.; Jung, G.; *Inorg. Chim. Acta* **1969**, 3, 69.
14. Ford, P. C.; Rokicki, A.; *Adv. Organomet. Chem.* **1998**, 28, 139, and references therein; Della Pergola, R.; Martinengo, S.; Manassero, M.; Sansoni, M.; *J. Organomet. Chem.* **2000**, 593, 63.
15. Fernandez, A. L.; Poë, A. J., unpublished observations on kinetics in partially and fully hydrated Na₅₆Y.
16. Oliveira, E. C. de; Pastore, H. O.; *Res. Chem. Intermed.* **2004**, 30, 857.

Received: June 4, 2007

Web Release Date: April 15, 2008

FAPESP helped in meeting the publication costs of this article.

Zeolite Activation of Organometallics: Revisiting Substitution Kinetics of [Mo(CO)₆] with Chemisorbed PMe₃ in Dehydrated Na₅₆Y Zeolite

Anthony L. Fernandez,^{,a} Jianbin Hao,^b Roberta L. Parkes,^b Anthony J. Poë^{*,b} and (the late) Eduardo J. S. Vichi^{c,#}*

^aDepartment of Chemistry, Merrimack College, 315 Turnpike Street, North Andover, MA 01845, USA

^bLash Miller Chemical Laboratories, University of Toronto, 80 St. George Street, M5S 3H6 Toronto, Canada

^cInstituto de Química, Universidade Estadual de Campinas, CP 6154, 13083-970 Campinas-SP, Brazil

Table S1. Rate constants^a for substitution reactions of [Mo(CO)₆] with chemisorbed PMe₃ in dehydrated Na₅₆Y under vacuum

T/(°C)	1975 cm ⁻¹ 10 ⁴ k _{obs} (err, χ ²) ^b	1865 cm ⁻¹ 10 ⁴ k _{obs} (err, χ ²) ^b
48	0.456 (13, 778)	0.517 (16, 136)
48	0.722 (17, 96)	0.600 (8, 58)
48	0.676 (2, 153)	0.600 (8, 58)
56	2.02 (36, 286)	1.54 (4, 170)
56	1.86 (4, 5)	1.48 (2, 19)
56	2.30 (9, 8)	1.42 (5, 34)
66	2.56 (3, 15)	2.50 (9, 38)
66	2.38 (6, 21)	2.30 (3, 20)
66	3.51 (6, 7)	3.46 (3, 7)
66	4.62 (14, 14)	3.58 (6,60)
66	3.08 (7, 8)	2.86 (3, 17)
75	5.42 (10, 3)	5.25 (8, 7)
75	6.69 (4, 25)	
85	9.45 (12, 158)	9.10 (32, 373)
85	10.3 (1, 1)	11.1 (2, 1)
85	14.3 (7, 3)	
85	15.5 (1, 1)	14.4 (2, 3)

^aRate constants obtained by fitting the time-dependent absorbances to single or double exponential functions

^b err = standard deviation of k_{obs}; χ² = goodness of fit (the smaller the number the better the fit). Thus 0.456(13, 778) represents 10⁴k_{obs} = 0.456 ± 0.013 s⁻¹ with χ² = 778.

[#] Professor Vichi sadly passed away just as this manuscript was being completed. Eduardo Vichi was the originator of the Intrazeolite Kinetics project. He suggested it to A.J.P. in Toronto in 1983 and eventually obtained funding for it through FAPESP and CNPq. He was a great scientific colleague and a warm friend, and he will be deeply missed.

*e-mail: anthony.fernandez@merrimack.edu; apoe@chem.utotonto.ca; anthonyapoe@rogers.com

Table S2. Rate constants^a for substitution reactions of [Mo(CO)₆] with chemisorbed PMe₃ in dehydrated Na₅₆Y under 650 Torr CO

T/(°C)	1975 cm ⁻¹ 10 ⁴ k _{obs} (err, χ ²) ^a	1865 cm ⁻¹ 10 ⁴ k _{obs} (err, χ ²) ^a
48	0.373 (9, 9319)	0.434 (5, 295)
48	0.395 (5, 2191)	0.475 (123, 56)
48	0.544 (18, 1090)	0.343 (4, 129)
48	0.420 (7, 708)	0.508 (4, 37)
		0.309 (3, 216)
56	0.601 (10, 2714)	0.910 (47, 279)
56	0.967 (162, 2087)	
56	0.687 (7, 412)	0.806 (15, 61)
56	1.65 (4, 4)	1.85 (4, 2)
56	0.766 (12, 67)	0.889 (18, 387)
56	1.10 (1, 110)	1.14 (1,15)
66	1.92 (9, 10)	3.86 (8, 23)
66	3.08 (15, 5)	2.01 (3, 5)
66	2.55 (2, 8)	
66	2.56 (4, 150)	3.10 (18, 466)
75	5.44 (12, 1819)	5.03 (2, 694)
75	6.38 (11, 5)	
85	12.0 (2, 1)	
85	19.2 (4, 1)	
85	12.2 (1, 1)	
85	11.6 (1, 2)	

^aRate constants obtained by fitting the time-dependent absorbances to single or double exponential functions

^b err = standard deviation of k_{obs}; χ² = goodness of fit (the smaller the number the better the fit). Thus 0.373(9, 9319) represents 10⁴k_{obs} = 0.373 ± 0.009 s⁻¹ with χ² = 9319.